frontiers | Frontiers in Ecology and Evolution

TYPE Original Research
PUBLISHED 29 September 2022
DOI 10.3389/fevo.2022.1016774

Spatiotemporal analysis of land use changes and their trade-offs on the northern slope of the Tianshan Mountains, China

Haitao Ma*

Key Laboratory of Regional Sustainable Development Modeling, Institute of Geographic Sciences and Natural Resources Research, Chinese Academy of Sciences, Beijing, China

The unprecedented urbanization recently has inevitably intensified the changes in land use morphology. However, current studies on land use primarily analyze a single morphology, ignoring the relationships between different land use morphologies. Taking the northern slope of the Tianshan Mountains (NSTM) as the study area, this article quantifies the spatiotemporal pattern of land use change, and estimates trade-offs and synergies between dominant (patch density, largest patch index, and landscape shape index) and recessive (land use efficiency, land use intensity, and agricultural non-point source pollution) morphologies to fully understand the dynamic characteristics of land use. Results showed bare areas and grassland were always predominant land use types, and land use change from 1990 to 2020 was characterized by the increase of impervious surfaces and the decrease of bare areas. The strongest trade-off was found between largest patch index and land use intensity, while the synergy between landscape shape index and land use intensity was strongest. There are significant disparities in terms of temporal and spatial patterns of trade-offs/synergies. The correlation coefficients in different study periods were much smaller than their estimations in the whole region, and the trade-offs/synergies in the eastern NSTM were basically identical with the whole relationships. The findings reveal the interactions among various land use characteristics, and provide significant references for coordinated land management and regional high-quality development.

KEYWORDS

land use change, trade-off and synergy, landscape pattern, dominant and recessive morphologies, the northern slope of the Tianshan Mountains (NSTM)

OPEN ACCESS

EDITED BY
Jun Yang,
Northeastern University, China

REVIEWED BY
Liang Jiao,
Northwest Normal University, China
Tiange Shi,
Xinjiang University of Finance and Economics, China
Huabin Xiao,
Shandong Jianzhu University, China

*CORRESPONDENCE
Haitao Ma
maht@igsnrr.ac.cn

SPECIALTY SECTION
This article was submitted to Environmental Informatics and Remote Sensing, a section of the journal Frontiers in Ecology and Evolution

RECEIVED 11 August 2022
ACCEPTED 12 September 2022
PUBLISHED 29 September 2022

CITATION
Ma H (2022) Spatiotemporal analysis of land use changes and their trade-offs on the northern slope of the Tianshan Mountains, China. *Front. Ecol. Evol.* 10:1016774. doi: 10.3389/fevo.2022.1016774

Introduction

Land systems are not only the surface covered by natural and artificial elements, but also the utilization of land by human beings. Land systems are complex and highly associated with climate change, food security, and regional inequality in the 2030 Agenda for Sustainable Development Goals (SDGs) (Fujimori et al., 2022; Meyfroidt et al., 2022; van Marle et al., 2022). This indicates that the efficient management and sustainable development of land systems will be of utmost importance to achieving SDGs in the following years. Recently, China has experienced unprecedented urbanization with increasing population, which inevitably intensifies the evolution of land systems (Zuo et al., 2018; Liu et al., 2021; He et al., 2022). Land use change refers to the transformation of land use morphology in a region during a certain period driven by human activities (Long et al., 2014). The concept of land use morphology was firstly proposed by Grainger (1995), who defined it as the overall pattern of actual land cover in a region at a given time. With the continuous social and economic changes, Long and Li (2012) enriched the connotation of the traditional quantity and distribution of land use morphology, and argued that land use morphology could be represented by dominant and recessive morphologies. Specifically, land use dominant morphology represents the directly visible features of land use, such as areas and spatial patterns, which is highly connected with the landscape patterns of land use. While land use recessive morphology refers to quality embodied in land use, such as property rights, functions, management mode, input, and output (Qu et al., 2021).

At present, studies of land use dominant morphology mainly focus on land use transition research (Long et al., 2021). Much attention had paid to the evolution of land use structure and the changes in the proportion of various land use categories (Ouedraogo et al., 2016; Buckley Biggs, 2022). They found that the proportions and areas of artificial land, especially urban construction land, gradually increased during the process of urbanization and industrialization, while those of natural land, such as forest, grassland, and unused land, displayed significant decreasing trends simultaneously. Some indices, such as gross gain, gross loss, and change rate, were also calculated to evaluate the temporal characteristics of land use during a certain period (Sumari et al., 2020; Duan et al., 2021; Chen et al., 2022). Recent empirical analysis validated the spatiotemporal differentiation of certain land use categories, primarily including cropland and impervious areas (Cai et al., 2020; Yang et al., 2021; Ray et al., 2022), and further discovered the hotspot characteristics of land use on the regional scale or explored the driving forces of land-use spatial distribution (Zhu et al., 2021). In terms of the studies of land use recessive morphology, scholars mainly concentrated on the changes in land use function (Schiavina et al., 2022). It was defined as goods and services provided by different land use categories in order to meet the demands of human activities. Considerable progress had identified land use function from the aspects of production, living, and ecology, by establishing a comprehensive index system (Meng et al., 2022). Besides, some literatures measured the degree of human activities on land use (Howison et al., 2018; Yin et al., 2020; Zhou et al., 2022), and captured the changes in fixed input or economic output efficiency per unit of land in a certain administrative region (Guo and Shen, 2015; Jiang et al., 2021).

Overall, most of the current studies on land use morphology primarily analyze a single morphology, but ignore the interactions between land use dominant and recessive morphologies. The loss of natural land not only reshapes the dominant landscape patterns of land use but also intensifies its recessive input and output. Natural land has consistently transferred into artificial land with the increasing human activities. The landscape patterns of land use became fragmented and dispersed over time. Simultaneously, the input and output embodied in land use increased sharply. There normally exists a positive correlation between dominant landscape patterns and recessive intensity of land use. In some certain cases, the dominant and recessive morphologies of land use do not present a positive correlation theoretically. For example, extensive management of land use has altered its dominant landscape patterns, but it does not bring corresponding economic benefits. Besides, some nature reserves take advantage of their abundant ecologic resources to attract sightseers without altering the dominant morphology of land use. It achieves a better combination of economic development and land protection. In summary, dominant and recessive morphologies of land use are concurrent, and it is of great importance to investigate their relationships to fully understand the dynamic characteristics of land use.

Nowadays, trade-off analysis has become an important method to manifest the relationships of multiple systems (Bradford and D'Amato, 2012). The trade-off is generally described as the status where a specific system benefits at the cost of others (Hamilton et al., 2019). A wealth of studies investigated the links and interactions among multiple natural ecosystem services (Howe et al., 2014; Cord et al., 2017; Geng et al., 2022), and some scholars recently explored the trade-offs/synergies between natural and artificial ecosystems such as multiple land use functions (Fan et al., 2021; Zhu et al., 2021; Meng et al., 2022), but it is relatively scarce to quantify the trade-offs and synergies of different land use characteristics. To fill this research gap, this article focused on the relationships between land use dominant and recessive morphologies. Taking the northern slope of the Tianshan Mountains (NSTM), an important developing area with a fragile environment in China, as the study area, we investigated the changes in land use and its landscape metrics based on land use data in 1990, 1995, 2000, 2005, 2010, 2015, and 2020. Next, the spatiotemporal characteristics of land use change in the NSTM from 1990 to 2020 were examined. Finally, land use dominant and recessive morphologies at the whole and county scales were estimated by incorporating land use and socio-economic datasets. On this basis, their trade-offs and synergies between land use morphology were qualified through Pearson correlation analysis. The findings contribute to revealing the interactions among various land use morphologies, and provide significant references for coordinated land management and regional high-quality development.

Materials and methods

Study area and data source

The northern slope of the Tianshan Mountains (NSTM) is located in the inland center of the Eurasian continent (Figure 1). It covers 79°53′E-96°23′E and 40°52′N-47°14′N with an area of three hundred and ninety-six thousand square kilometers, accounting for 23.8% of the total area of Xinjiang Uygur Autonomous Region. The terrain, ranging from −192 to 5,166 m, is high in the Tianshan Mountains and low in the surrounding basins. The NSTM includes areas of Urumqi City, Karamay City, Bortala Mongol Autonomous Prefecture, Changji Hui Autonomous Prefecture, Hami City, Tacheng Administrative Office, Turpan City, Kuytun City, and four county-level cities (i.e., Shuanghe City, Wujiaqu City, Huyanghe City, and Shihezi City). The NSTM is the main area of urbanization and economic development in the autonomous region, whose GDP accounts for more than 60% of that in Xinjiang. The NSTM has a typical continental climate with hot-dry summer and cold-long winter, and the temperature

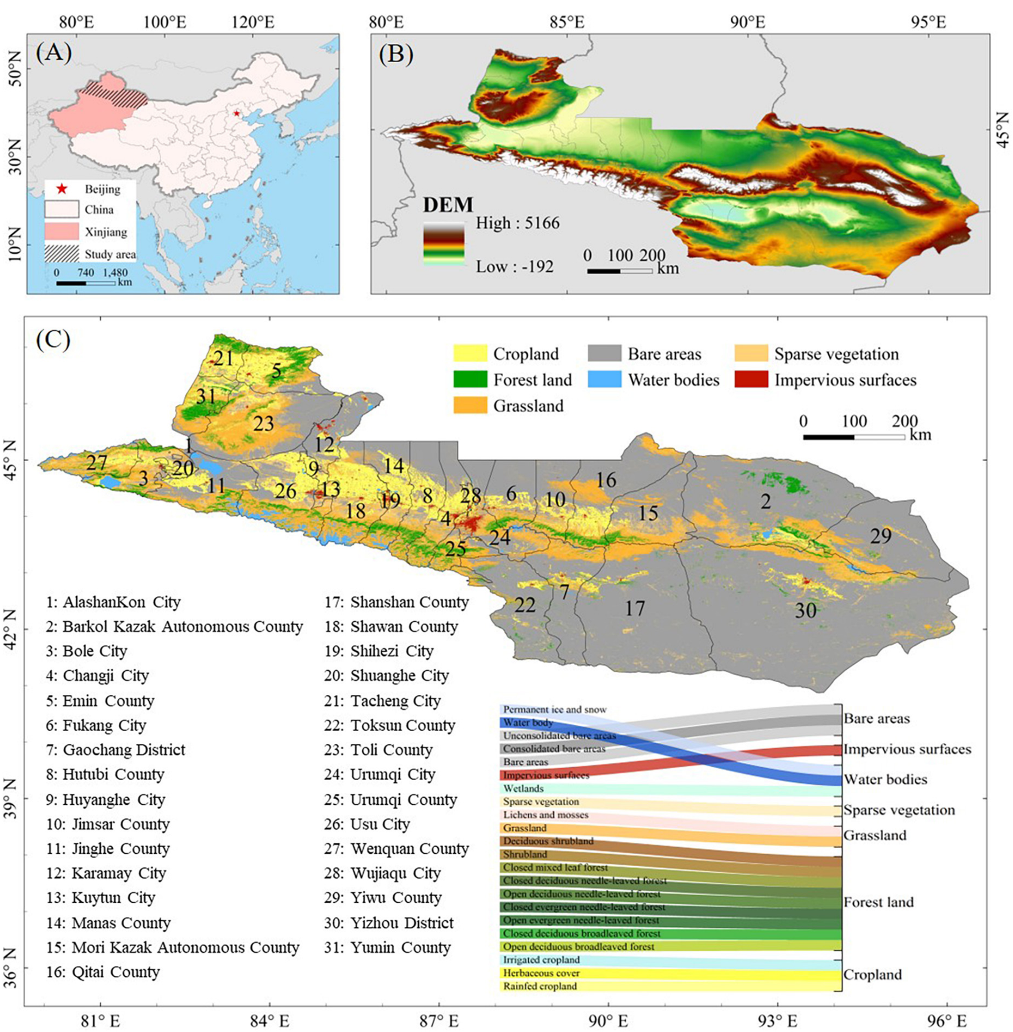

FIGURE 1
(A) The location of the NSTM. **(B)** The elevation of the NSTM derived from the ASTER Global Digital Elevation Model at 30 m, and downloaded from the Geospatial Data Cloud of China. **(C)** The spatial patterns of land use of the NSTM in 2020 derived from GLC_FCS30. The corresponding relationships between the land use classification used in this study and the original system of the dataset are also depicted.

changes greatly from morning to night, and its annual average temperature is 6–7.2°C. The annual average precipitation ranges from 20 to 400 mm, but the annual evaporation amount reaches 1,817 mm. Geological feature is mainly characterized by limestone, sedimentary rock, carbonate, and silicate rock in the NSTM. There are various soil types in the NSTM, including gray brown desert, brown soil, chestnut, chernozem, gray cinnamon, and meadow soil.

Data used in this study are primarily obtained in two ways. Firstly, the Global land-cover product with fine classification system at 30 m (GLC_FCS30) is employed in the study due to its high spatial resolution and long time series, which is freely available at https://doi.org/10.5281/zenodo.3986872. Validation results have shown the overall accuracy and kappa coefficient of this product are 0.825 and 0.784 in terms of nine major land-cover types, which is higher than GlobaLand30 and FROM_GLC products. This dataset, extracted from Landsat remote sensing images and high-quality training data from Global Spatial Temporal Spectra Library, provides a detailed classification system containing 29 land cover types (Zhang X. et al., 2021). Considering the land use structure of the study area, a new classification system is established by reclassing land use types into seven groups: cropland, forest land, grassland, water bodies, bare areas, sparse vegetation, and impervious surfaces. The data processing of land use was implemented using ENVI 5.3 and ArcGIS 10.8 software platform. The land use data every 5-year interval (i.e., 1990, 1995, 2000, 2005, 2010, 2015, and 2020) are employed to identify the changes in land use morphology. According to the land cover of the NSTM in 2020, land cover type displayed obvious divergence in the study area. Specifically, cropland was mainly distributed in the north of the study area, while forest land, grassland, and sparse vegetation were roughly distributed along the Tianshan Mountains due to elevation gradients. Bare areas were the largest land surface cover, accounting for 61.2% of the total area, which was distributed in the eastern study area. The distributions of water bodies were scattered, including Sayram Lake, Ebinur Lake, and Kashgar River Basin. Impervious surfaces were mainly distributed in the center of Urumqi City, Shihezi City, Kuytun City, Karamay City, and other cities. Secondly, socio-economic data are collected from the Xinjiang Uygur Autonomous Region[1] and their affiliated districts and counties.

Land use change indices

Land use change indices have been used to quantify the characteristics of land use change during a certain period (Sumari et al., 2020; Duan et al., 2021). The gross gain and gross loss are the most basic components at the category level. They are calculated as follows:

$$G_i = P_{+i} - P_{ii} \tag{1}$$

$$L_i = P_{i+} - P_{ii} \tag{2}$$

where G_i denotes the gross gain of category i during a certain period, which is given by P_{+i} minus P_{ii}. L_i denotes the gross loss of category i during a certain period, which is given by P_{i+} minus P_{ii}. P_{+i} and P_{i+} are the percentage of the area in category i at the final time and the initial time of a certain period, respectively. P_{ii} represents the area that shows the persistence of category i.

Based on the above two basic components, other components of land use change can be estimated: net change, swap change, total change, and change rate (Chen et al., 2022). The net change shows the change percentage of a certain land use type during the study period, which is given by the gross gain minus the gross loss. The calculation formula is:

$$N_i = G_i - L_i = P_{+i} - P_{i+} \tag{3}$$

where N_i is the net change of category i during a certain period.

The swap change is quantitatively calculated by twice the minimum of the gross gain and the gross loss, which is expressed as follows:

$$S_i = 2 \times \min(G_i, L_i) \tag{4}$$

where S_i is the swap change of category i during a certain period.

The total change reflects the sum of changed areas of a certain land use type during the study period. The calculation formula is as follows:

$$T_i = G_i + L_i \tag{5}$$

where T_i is the total change of category i during a certain period.

The change rate represents the changing trend of a certain land use type during the study, which is expressed as follows:

$$R_i = \frac{N_i}{P_{i+}} \tag{6}$$

where R_i is the change rate of category i during a certain period.

Land use morphology indices

Land use change refers to the spatiotemporal changes in land use morphology driven by social and economic development. It is acknowledged that there are two formats to describe land use morphology, i.e., dominant morphology and recessive morphology (Long and Li, 2012).

Dominant morphology

Landscape pattern indicators have been widely used to analyze landscape composition and spatial structure among

1 http://tjj.xinjiang.gov.cn/

patches within a category or region level (Lausch et al., 2015; Li et al., 2017; Yang et al., 2019; Sumari et al., 2020; Müller et al., 2022). Land use change is always accompanied by changes in landscape characteristics, which has directly transformed the landscape fragmentation, concentration, and connectivity. Therefore, the dominant morphology is quantitatively estimated by landscape pattern indicators in this study. In accordance with previous studies (Ma et al., 2019; Wu and Lu, 2021; Fu et al., 2022), patch density (PD), largest patch index (LPI), and landscape shape index (LSI) are selected and calculated using the Fragstats 4.2 software. Kubacka et al. (2022) have also proved there are no strong relationships among PD, LPI, and LSI, which can overcome multivariable multicollinearity in terms of different indicators and provide reliable information to explore the land use dominant morphology. The definitions and calculation formulas of the selected landscape metrics are listed in **Table 1**.

Recessive morphology

Studies of land use recessive morphology mainly concentrated on the changes in land use efficiency (Jiang et al., 2021; Schiavina et al., 2022), land use intensity (Tan et al., 2022; Zhou et al., 2022), and its environmental effects (Searchinger et al., 2018; Hong et al., 2021; DeFries et al., 2022; van Marle et al., 2022). The efficiency of land use directly reflects the level of socio-economic development (Yu et al., 2019). Compared with the primary industry, manufacturing and service industries are more efficient and productive obtained from land use. Land use efficiency (LUE) is expressed as the economic output per unit of land in this study. Land use intensity (LUI) is employed to evaluate the status of land development within a region. Referring to Xu et al. (2020), a specific weight value is assigned to each basic land use type by considering the extent of human activities and fixed inputs. Seven land use types are reclassed into five new groups: high-use-intensity artificial land, low-use-intensity artificial land, high-use-intensity natural land, mid-use-intensity natural land, and low-use-intensity natural land. The LUI index is calculated by the weighted sum of each reclassed group. Agricultural system, accounting for about 30% of global greenhouse gasses, is a major source of climate change (Clark et al., 2020; Foong et al., 2022; Wang et al., 2022). Agricultural non-point source pollution (ANSP) caused by intensive chemical fertilizer consumption greatly contributes to the decline of ecological environment, and further threatens food security in the country (Zhang Y. et al., 2021; Plunge et al., 2022). Therefore, the chemical fertilizer consumption per cropland area is employed to represent the environmental effects of land use. The definitions and calculation formulas of the selected variables are listed in **Table 2**.

Trade-off/synergy analysis

Based on the long-time series data from 1990 to 2020, the relationships between land use dominant and recessive morphologies are evaluated using correlation analysis. Compared with other methods, like Spearman correlation analysis, Pearson correlation analysis is capable of capturing information embedded in the sample data, and has been widely used in the relationships between two variables (Zhu et al., 2021; Bai et al., 2022; Ren et al., 2022). Pearson correlation analysis is employed and the calculation formula is as follows:

$$r(X_i, Y_i) = \frac{\sum_{i=1}^{N}(X_i - \overline{X})(Y_i - \overline{Y})}{\sqrt{\sum_{i=1}^{N}(X_i - \overline{X})^2 \sum_{i=1}^{N}(Y_i - \overline{Y})^2}} \quad (7)$$

where $r(X_i, Y_i)$ represents the Pearson correlation analysis between X and Y. X_i and Y_i are the estimated value of land use dominant and recessive morphologies in region i. $\overline{X}$ and $\overline{Y}$ are their average values, respectively. N is the number of regions.

We used the Stata 16 software to estimate the correlation coefficients (r) and significance tests (P). The positive coefficient represents a trade-off relationship between different indicators, meaning both land use morphologies increase or decrease simultaneously. Otherwise, a synergy relationship occurs when the coefficient is negative, indicating an increase in one land use morphology leads to the decrease in another. In this regard, the relationships between land use dominant and recessive morphologies are classified into seven types: high synergy ($r > 0$, $P < 0.01$), middle synergy ($r > 0$, $0.01 < P < 0.05$), low synergy ($r < 0$, $0.05 < P < 0.1$), high trade-off ($r < 0, P < 0.01$),

TABLE 1 Description of land-use dominant morphology index.

Index	Significance	Formula
PD	PD reflects the degree of landscape fragmentation. It is calculated by the number of patches involving the corresponding patch type divided by the total landscape area.	$PD = \frac{n_i}{A_i}$
LPI	LPI reflects the concentration degree of patches. It is calculated by the largest patch of the corresponding patch type divided by the total landscape area.	$LPI = \frac{max a_{ij}}{A_i}$
LSI	LSI reflects the degree of shape complexity. It is calculated by 0.25 times the total length of edge divided by the square root of the total landscape area.	$LSI = \frac{0.25E_i}{\sqrt{A_i}}$

n_i is the number of patches of category/region i. A_i is the total landscape area of category/region i. a_{ij} is the area of patch j of category/region i. E_i is the total length of the edge of category/region i.

TABLE 2 Description of land-use recessive morphology index.

Index	Significance	Formula
LUE	LUE reflects the economic output of land use, which is accompanied by the level of socio-economic development. It is calculated by the output of GDP in a certain region divided by its corresponding impervious area.	$LUE = \frac{GDP_i}{A_{iI}}$
LUI	LUI reflects the degree of human activities on land use. It is calculated by the sum of each land-use group multiplied by its weight value.	$LUI = \sum_{j=1}^{5} \frac{A_{ij}}{A_i} \cdot W_j$
ANSP	ANSP reflects the environmental effects of land use. It is calculated by the chemical fertilizer consumption per cropland area, that is, the consumption of chemical fertilizer in a certain region divided by its corresponding farmland area.	$ANSP = \frac{CFC_i}{A_{iF}}$

GDP_i is the output of GDP of region *i*. A_{iI} and A_{iF} are the impervious area and farmland area of region *i*, respectively. A_i is the total area of region *i*. A_{ij} is the area of group *j* in region *i*. W_j is the weight value of group *j*. The weight values of high-use-intensity artificial land (i.e., impervious surfaces), low-use-intensity artificial land (i.e., cropland), high-use-intensity natural land (including forest land, grassland, and water bodies), mid-use-intensity natural land (i.e., sparse vegetation), and low-use-intensity natural land (i.e., bare areas) are set to 5, 4, 3, 2, and 1, respectively. CFC_i is the chemical fertilizer consumption of region *i*.

middle trade-off ($r < 0$, $0.01 < P < 0.05$), low trade-off ($r < 0$, $0.05 < P < 0.1$), and insignificance ($P > 0.1$).

Results

Land use and landscape characteristics in the northern slope of the Tianshan Mountains

The proportions of land use types and their changes from 1990 to 2020 are shown in **Figure 2**. Overall, though the proportion of each land use type changed over time, the order of their proportions approximately remained the same. Bare areas and grassland were always predominant land use types from 1990 to 2020 in the NSTM, and their proportions both showed downward trends over time. The proportions of impervious surfaces and water bodies always were in the last two land use types in the NSTM, and their values both displayed upward trends over time. Specifically, bare areas decreased from 64.89 to 61.20% from 1990 to 2020, while impervious surfaces gradually and consistently increased from 0.33 to 0.77%. The trends of cropland, sparse vegetation, and forest land increased in fluctuation.

The landscape patterns of each land use type from 1990 to 2020 were obtained (**Figure 3**). The PD of sparse vegetation and grassland were largest, and their values exhibited increasing trends over time. Water bodies and impervious surfaces had lower PD than other land use categories, and they were basically unchanged during the study period. According to the results of LPI, bare areas had the largest values mainly due to their vast areas, and their values were 10 times more than others. There existed substantial differences in LPI among different land use types. As for the LSI at the category level, sparse vegetation and grassland ranked as the top two among various land use types, while water bodies and impervious surfaces were low. The values of six categories (except cropland) displayed increasing trends from 1990 to 2020. Overall, the LPI of various land use types were roughly proportional to their areas. The PD and LSI of cropland showed a decreasing trend, while the values of LPI increased over time, indicating the cropland in the NSTM gradually became concentrated and integrated in the past three decades. The values of water bodies and impervious surfaces were low in terms of three landscape metrics, mainly due to their small areas. But impervious surfaces had larger PD and LSI, and smaller LPI than water bodies, indicating that impervious surfaces were more dispersed and fragmented in the NSTM.

Temporal and spatial patterns of land use change in the northern slope of the Tianshan Mountains

Four variables, i.e., net change, swap change, total change, and change rate, were evaluated to identify the land use change at the category level during the 5-year intervals (**Figure 4**). Land use categories with larger proportions, such as bare areas and grassland experienced the net losses during all intervals. The areas of forest land and cropland experienced a slight net loss in the last decade. The net changes of impervious surfaces from 1990 to 2020 were always positive, indicating the areas of impervious surfaces increased consistently. As for the swap change index, bare areas, grassland, and sparse vegetation experienced the largest values, followed by cropland, then forest land and water bodies. It should be noticed that the swap changes of impervious surfaces were nearly zero because impervious surfaces were hardly transferred out. The larger the land use category areas, the larger their total changes. The total change of bare areas was largest among various land use types. Land use categories with small proportions, such as water bodies and impervious surfaces, and experienced very small total changes. The change rates of impervious surfaces were above 10% during all intervals, and the fastest period was from 2000 to 2005, of which the value was 25.18%. The change rates of bare areas and grassland were negative from 1990 to 2000. Though the net loss of bare areas was greater than those of

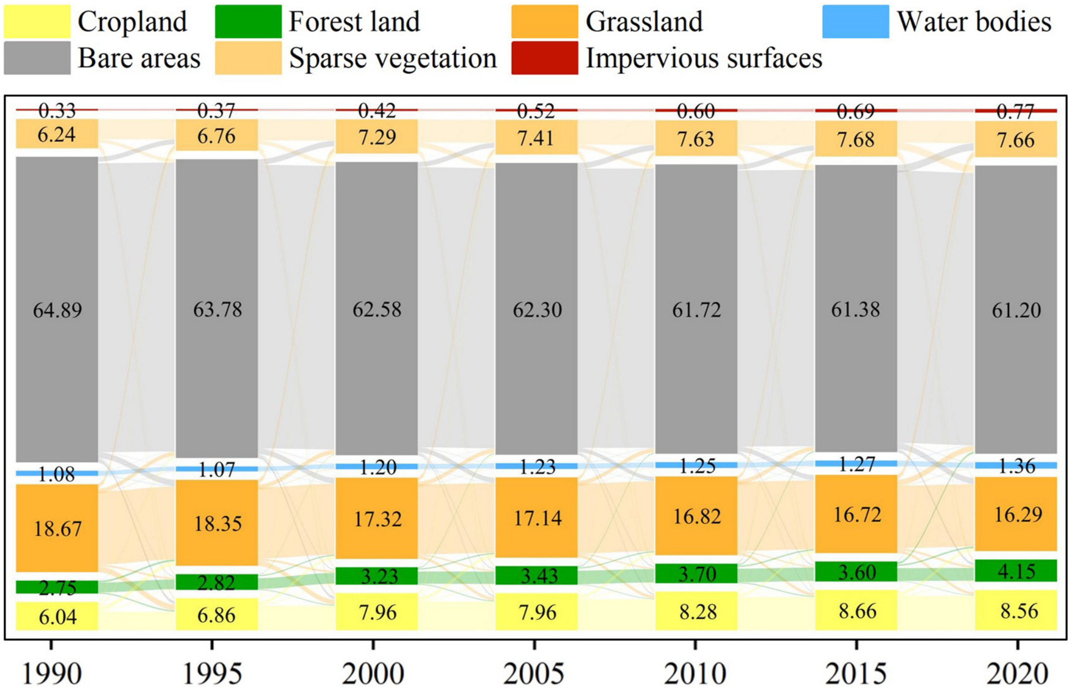

FIGURE 2
Sankey plot of land use change in the NSTM. Stacked vertical bars represent the proportions of various land use types from 1990 to 2020. Lines between each pair of bars visualize the changes of each land use type in the 5-year interval. The thickness of each line represents the proportion of the corresponding land-use area that experiences the persistence or transition.

grassland, the change rates of bare areas were smaller due to their high proportion and vast areas.

To clearly understand the general condition of land use change in the NSTM, temporal and spatial patterns of land use change from 1990 to 2020 were depicted. According to the estimated results in **Figures 5A,C**, more than 20% of the total area in the NSTM experienced land use change, and the transformations of bare areas, grassland, and sparse vegetation were predominant during the past three decades.

From the perspective of outflow based on land use structure in 1990 (**Figures 5A,B**), 41.51% of cropland had transformed into other land use categories in 2020, primarily including grassland, sparse vegetation, and bare areas, which mainly covered Jimsar County, Urumqi City, Urumqi County, Changji City, and so on. 25.60% of forest land had transformed into other land use categories, primarily including grassland, cropland, and bare areas, which mainly covered Yumin County, Tacheng City, Jinghe County, Shuanghe City, and so on. 35.41% of grassland had transformed into other land use categories, primarily including cropland, sparse vegetation, and bare areas, which mainly covered Toli County, Emin County, Usu City, Wenquan County, and so on. 54.51% of sparse vegetation had transformed into other land use categories, primarily including bare areas, cropland, and grassland, which mainly covered Mori Kazak Autonomous County, Qitai County, Hutubi County, Shihezi City, and so on. 11.30% of bare areas had transformed into other land use categories, primarily including sparse vegetation, grassland, and cropland, which mainly covered Yizhou District, Barkol Kazak Autonomous County, Gaochang District, Usu City, Kuytun City, and so on. 19.03% of water bodies had transformed into other land use categories, primarily including grassland, and bare areas, mainly covering Ebinur Lake Watershed in Jinghe County. Only 0.07% of impervious surfaces in 1990 had transferred into other land use categories in 2020.

From the perspective of inflow based on land use structure in 2020 (**Figures 5C,D**), 58.76% of cropland had been transferred from other land use categories in 1990, primarily including grassland (22.23%), bare areas (20.61%), and sparse vegetation (13.69%), which mainly covered Tacheng City, Emin County, Shawan County, Usu City, and so on. 50.71% of forest land had been transferred from other land use categories, primarily including grassland, and bare areas, which mainly covered Changji City, Hutubi County, Urumqi County, Barkol Kazak Autonomous County, and so on. 25.95% of grassland had been transferred from other land use categories, primarily including bare areas, cropland, and sparse vegetation, which mainly covered Toli County, Urumqi County, Jimsar County, Shawan County, and so on. 62.95% of sparse vegetation had been transferred from other land use categories, primarily including

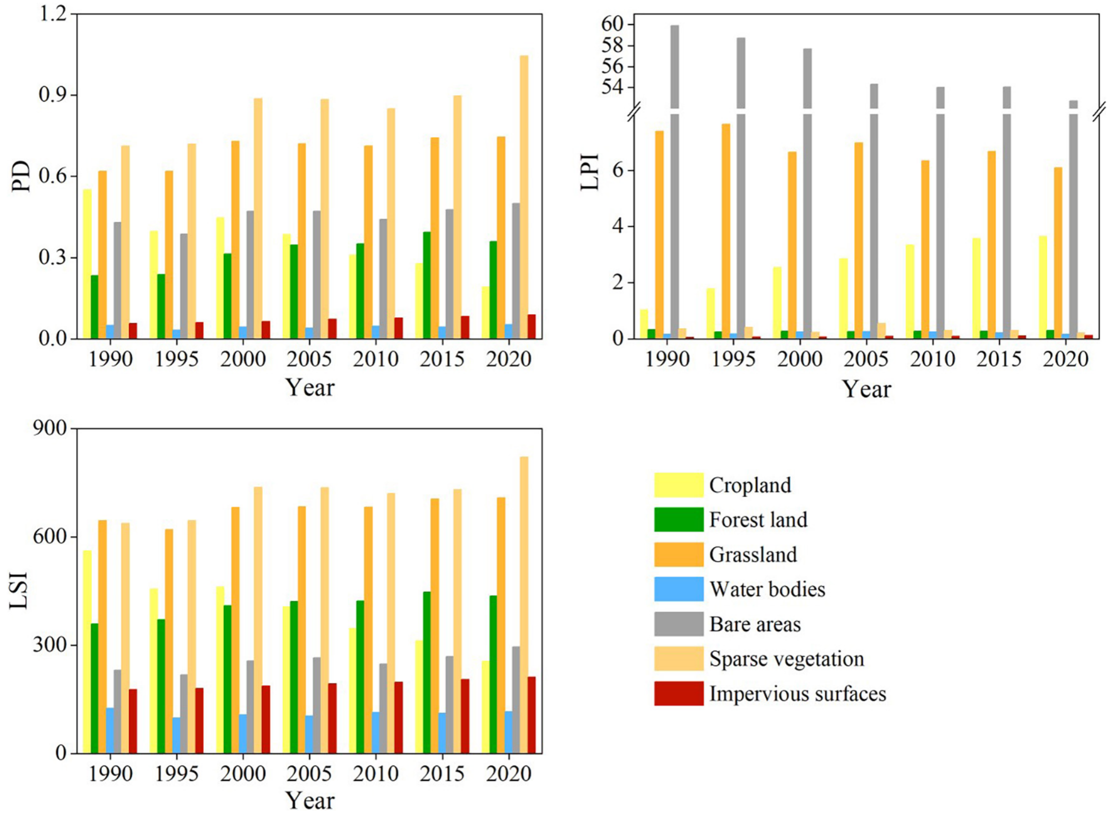

FIGURE 3
The changes in landscape metrics at the category level from 1990 to 2020.

bare areas, grassland, and cropland, which mainly covered Yizhou District, Shanshan County, Wenquan County, Yumin County, and so on. 5.97% of bare areas had been transferred from other land use categories, primarily including grassland and sparse vegetation, which mainly covered Jinghe County, Bole City, Mori Kazak Autonomous County, Urumqi City, and so on. 35.59% of water bodies had been transferred from other land use categories, primarily including grassland, and bare areas, mainly covering Barkol Kazak Autonomous County and the Kashgar River Basin. 57.09% of impervious surfaces had been transferred from other land use categories, primarily including cropland, bare areas, and grassland, which mainly covered Urumqi City, Changji City, Yiwu County, Kuytun City, and so on.

Trade-off and synergy of land use morphology

Trade-off and synergy analysis in the whole region

We quantified the temporal patterns of land use dominant and recessive morphologies from 1990 to 2020 in the NSTM using land use and socio-economic datasets. On this basis, the trade-offs and synergies between land use morphology in the whole region were estimated. Figure 6 shows the temporal changes in land use dominant and recessive morphologies in the NSTM. The whole PD decreased from 2.65 in 1990 to 2.45 in 1995, and fluctuated from 2.79 to 2.98 after 2000. The whole LPI displayed a consistent downward trend, decreasing from 59.90 in 1990 to 52.71 in 2020. The temporal trend of LSI was more complicated than PD and LPI. LPI reached its lowest value in 1995, which was similar to that of PD. It decreased in the first decade of the new century and increased in the following decade, whose largest value occurred in 2020. As for land use recessive morphology, the whole LUE displayed an increasing trend during the past three decades, meaning land use in the NSTM became more efficient and productive. It increased from 0.91 in 1990 to 21.33 in 2020, and this upward trend gradually increased in strength over time. The whole LUI also showed an upward trend over time, increasing from 1.71 in 1990 to 1.80 in 2020. The whole ANSP increased significantly from 1990 to 2005, and fluctuated between 248.89 and 386.03 during the following years.

The trade-offs and synergies between land use morphology in the whole region are presented in Figure 7. The strongest

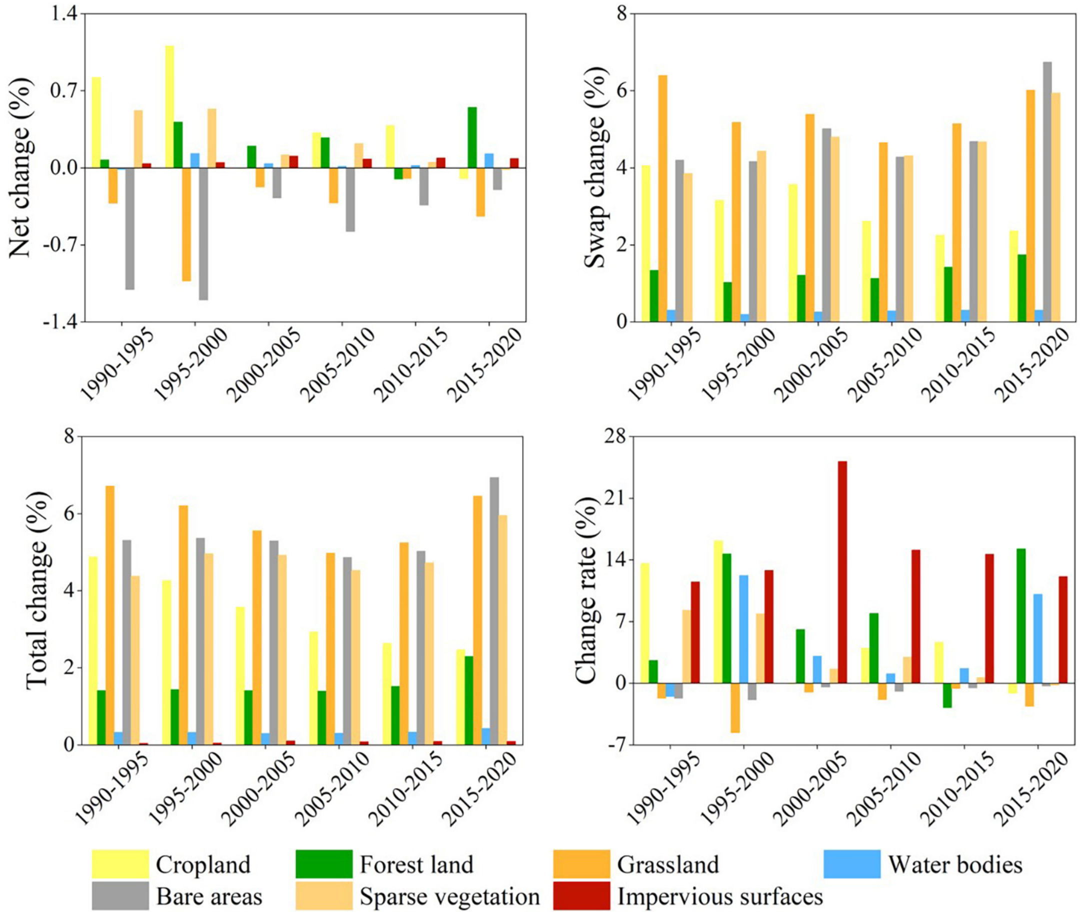

FIGURE 4
The land use change indices at the category level of the NSTM during the 5-year intervals.

trade-off relationship occurred between LSI and LUI, while the synergetic relationship between LPI and LUI was strongest, indicating the degree of human activities on land use was highly connected with land use dominant morphology index. The correlation coefficient between PD and LUE was positive and insignificant, indicating there was no significant synergetic relationship between landscape fragmentation and economic output of land use in the NSTM. The correlation coefficients between LPI and LUE as well as ANSP were significantly negative at the 5% level, which meant the degree of shape complexity displayed the strong trade-off relationships with the economic output and environmental effects of land use. The correlation coefficients between PD and LUI as well as ANSP were significantly positive at the 10% level, indicating the degree of landscape fragmentation had synergetic relationships with human activities and environmental effects of land use. The correlation coefficients between LSI and LUE as well as ANSP were also significantly positive at the 10% level, meaning the concentration degree of patches had synergetic relationships with the economic output and environmental effects of land use.

Trade-off and synergy analysis at the county level

In this section, we firstly explored their trade-off and synergetic relationships in 1990, 1995, 2000, 2005, 2010, 2015, and 2020 using land use morphology estimations at the county level, as presented in **Figure 8**. The relationships between dominant and recessive morphologies of land use exhibited significant disparities over time, and the correlation coefficients in different study periods were much smaller than their estimations in the whole region. The relationships between LSI and LUE were consistently negative in all periods, indicating a county with a high degree of shape complexity was inclined to decrease its economic output of land use. The correlation coefficients of PD and LUI were negative, while LPI and LUI displayed positive relationships from 1990 to 2020. It meant the counties with lower fragmentation and higher concentration of patches were prone to experiencing high-intensity human activities, which contributed to the improvement of labor productivity under large-scale and intensive production. However, the trade-off and synergetic

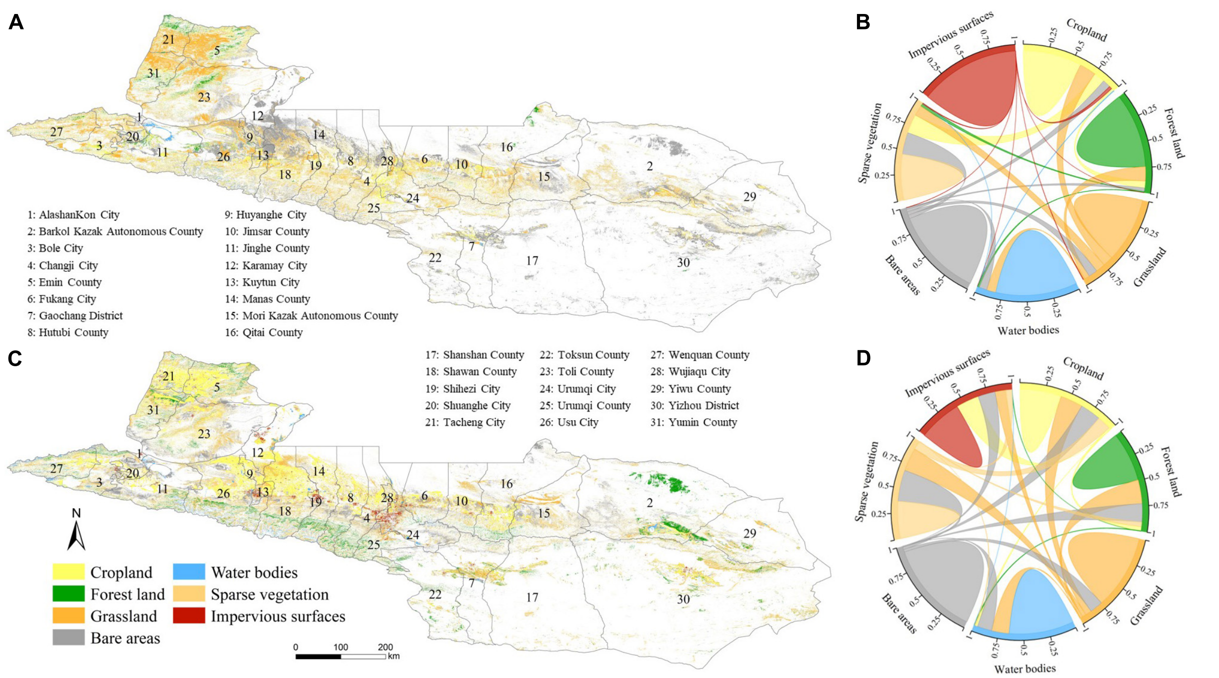

FIGURE 5
Land use change from 1990 to 2020 in the NSTM. The spatial distribution **(A)** and its outflow proportion **(B)** of each category to other categories based on land use structure in 1990. The spatial distribution **(C)** and its inflow proportion **(D)** of each category from other categories based on land use structure in 2020.

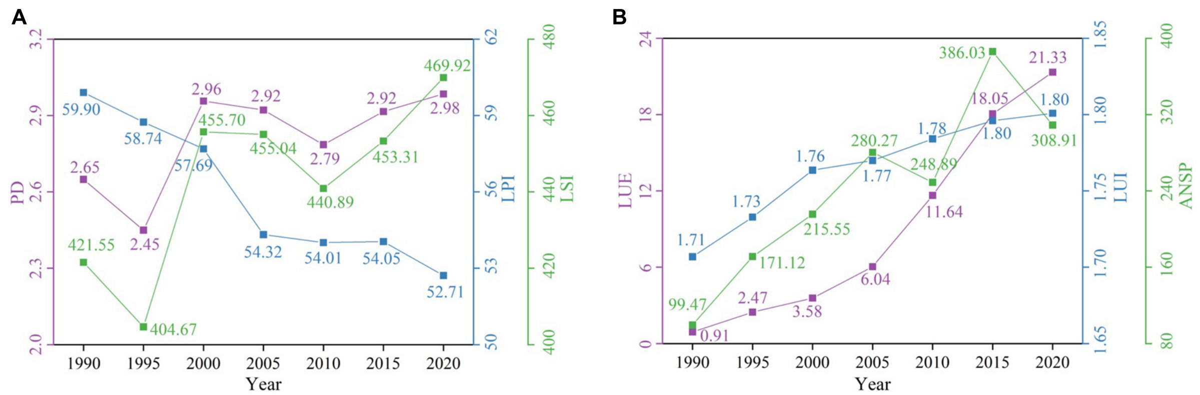

FIGURE 6
(A) The changes in global land use dominant morphology from 1990 to 2020 in the NSTM. **(B)** The changes in global land use recessive morphology from 1990 to 2020 in the NSTM.

relationships of other land use morphology indicators were up and down over time, which means different counties in the NSTM exhibited their individual characteristics, so there was no fixed relationship between land use dominant and recessive morphologies.

Moreover, distinct spatial patterns of various counties were identified through the trade-off analysis, as shown in Figure 9. There are significant disparities in terms of spatial patterns of trade-offs/synergies. The relationships in the east of the NSTM were basically identical with the whole region. A possible reason was that eastern counties, including Yizhou District, Shanshan County, Barkol Kazak Autonomous County, and Mori Kazak Autonomous County, are located at the Turpan Hami basin with vast desert and Gobi, and their proportion of bare areas was 20% higher than the average value according to the land cover in 2020. The supply of artificial land was insufficient for the demand of increasing population, so natural land had transformed into impervious surfaces to

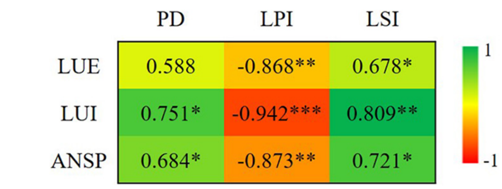

FIGURE 7
The global trade-offs/synergies between dominant and recessive morphologies of land use in the NSTM. *, **, and *** denote the significance level of 0.1, 0.05, and 0.01, respectively.

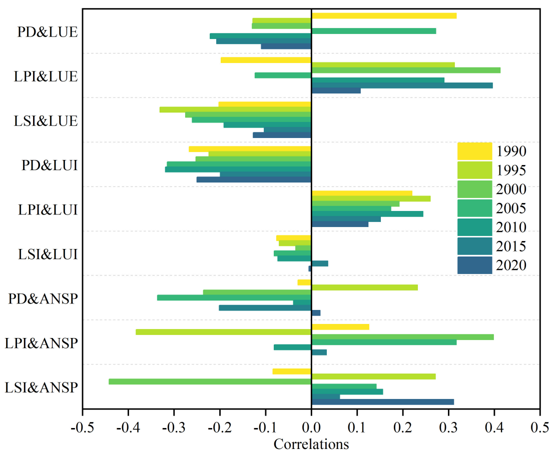

FIGURE 8
The temporal patterns of trade-offs/synergies between land use dominant and recessive morphologies.

promote economic development, which was consistent with the characteristics of land use in the whole region. However, the middle-south regions, including Huyanghe City, Kuytun City, Shawan County, and Usu City, displayed the opposite relationships with the NSTM. It was found that the infilling type of land use was dominant in these counties, representing the newly added patches were filled into or spread along the edge of the old land patches. The temporal patterns of PD and LSI decreased over time, while LPI increased. One explanation for this phenomenon could lie in the geographical conditions of these counties. They are located at the foot of Tianshan Mountains with smooth terrain, and there are sufficient water resources provided by rivers and streams, which is instrumental in mechanized operations, so their land use morphology became compact and integrated over time. Besides, some counties, including Bole City, Fukang City, Jinghe County, Manas County, Qitai County, and Wenquan County, showed insignificant relationships between land use dominant and recessive morphologies. Though the economic output and fertilizer input of land use significantly increased in the past three decades, their land use structure changed slightly, and land use dominant landscape patterns experienced minor changes within a small range. Therefore, the correlation coefficients between land use morphology in these counties were insignificant.

Discussion

This study explored the spatiotemporal patterns of land use and landscape changes, and the trade-offs of land use morphology. The NSTM has experienced rapid economic development over the past decades, leading to extensive land use and insufficient land supply. The proportion of cropland increased in fluctuation, and its change rate was much lower than that of impervious surfaces. One reason for this phenomenon was that the improvement of agricultural technology greatly increased crop production efficiency, and less cropland was required to achieve the food demand brought by the increasing population (Coomes et al., 2019). Another reason could lie in the extensive utilization of construction land. It is acknowledged that the pace of land-oriented urbanization is faster than that of demographic urbanization (Long et al., 2021). The areas of forest land increased recently mainly due to the implementation of environmental protection policies, and the ecological function of land use has gained more and more attention nowadays (Ma et al., 2019; An et al., 2022). It should be noticed that the land use in the NSTM became more fragmented over time according to the changes in landscape patterns, which pose serious threats to the efficient utilization and sustainable development of land systems.

The changes in land use dominant morphology presented the landscape complexity increased in the NSTM, and land use became more fragmented and dispersed over time. The whole LPI was determined by the largest patch of bare areas. Vast bare areas transformed into other land use categories in the context of agricultural development, thus decreasing its patch areas. Besides, in the initial stages of economic development before 1995, the old land use type was primarily filled up with new patches, and land use morphology became compact. Then the outlying type became predominant during the period of 1995–2000, and the degree of landscape fragmentation and shape complexity in the NSTM greatly increased. After the implementation of China's western development strategy in 2000, the landscape patterns of land use showed a volatile trend over time. The whole LUE and LUI increased due to the consistent transformation from natural land to artificial land and its GDP increased from 16.63 billion yuan in 1990 to 903.47 billion yuan in 2020. Compared with the trend of LUE, the upward trend of LUI gradually became slight over time. It was mainly because technological innovations and management practices had significantly promoted the quality of land use with fewer land resource utilization (Tan et al., 2021). The change in ANSP lied in the fact modern agricultural mechanization with high fixed costs was less effective in smallholder farms. Previous

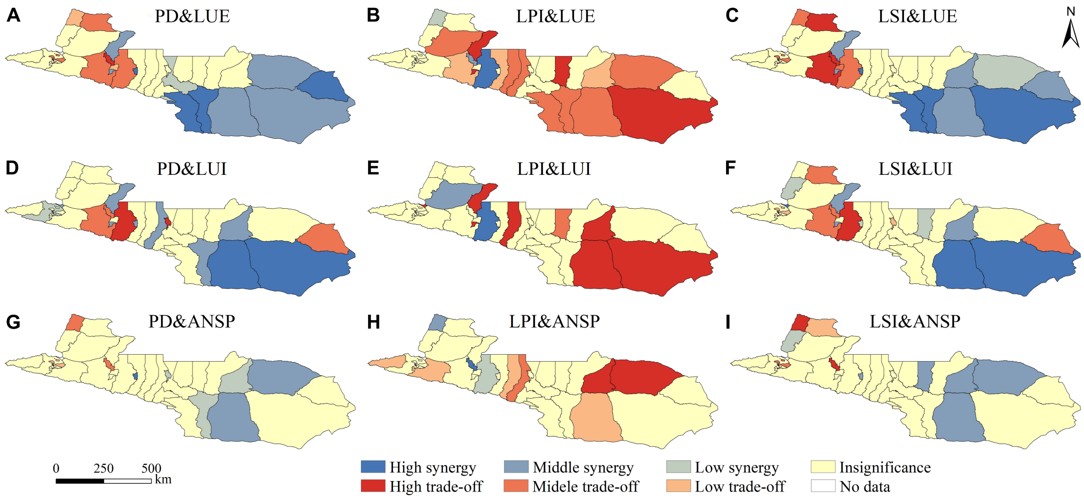

FIGURE 9
The spatial patterns of trade-offs/synergies between each pair of land use dominant and recessive morphology indices. Alashankou City was set in 2012, so the indices based on statistical data (LUE and ANSP) before its establishment is unavailable, which is denoted using blank space.

study has also shown that Chinese cropland was featured by smaller farm size and more agricultural chemicals than others (Wu et al., 2018). Besides, China has implemented the cultivated land occupation-supplement policy balance to ensure food security since 1997. Cultivated land was compensated by land exploitation, and the quantity balance was met. But urban expansion occupied highly productive cropland, and the quality had decreased sharply (Cai et al., 2020). Therefore, farmers were inclined to use more chemical fertilizers to increase crop yields. In recent years, some advanced technologies, such as soil testing, have been adopted to control agricultural pollution under China's ecological civilization construction.

Based on the trade-offs and synergies of land use morphology, several implications are proposed for high-quality development in the NSTM. Turpan Hami basin in the south of the NSTM, including Gaochang District, Toksun County, Shanshan County, Barkol Kazak Autonomous County, Mori Kazak Autonomous County, and Yizhou District, exhibits a synergetic relationship between PD and LSI and three recessive morphology indices, are key ecological zones. These regions are mainly covered by bare areas with fragile ecological environments and scarce water resources, and are vulnerable to land desertification, so their primary goals are to protect biodiversity, conserve water, and prevent desertification (An et al., 2022). County-level cities are relatively scattered in the NSTM through establish cities in the Gobi. Landscape fragmentation displayed a consistently increasing trend in Shihezi City during the past three decades, and land use morphology became more complex with the expansion of construction land boosted by industrial structure optimization. The role of these regions is to maintain the stability of the border regions. Urumqi City, the economic center of the NSTM, should take full advantage of its economy and location strength to form the innovation-oriented development mode and strengthen its spillover effect on surrounding regions. Overall, being an important location of the Belt and Road Initiative, infrastructure construction in the NSTM should be improved to strengthen commercial and cultural links with other regions, and take advantage of their cultural and tourism resources.

There are three prospective directions for this study that could be further explored in the future. First, this study identified the patterns of land use changes and their trade-offs, but it ignores the driving mechanism of land use by integrating geographical features and socio-economic indicators, which requires further exploration in future research by considering quantifiable influencing forces to enhance its accuracy and reliability. Second, it is meaningful to establish a systematic evaluation index system through an in-depth exploration of the relationship between land use dominant and recessive morphologies, which is helpful to explore various land use modes for regional high-quality development. Finally, the historical land use change in the past three decades was evaluated. Future studies should predict the land use changes in the following years under various development scenarios, and further understand its effects on climate change, biological diversity, and so on (Bukovsky et al., 2021; Huang et al., 2022; Li et al., 2022).

Conclusion

Taking the NSTM, an important developing area with a vulnerable environment in China, as the study area, this study investigated the changes in land use and its landscape metrics based on land use data in 1990, 1995, 2000, 2005, 2010, 2015, and 2020. Next, land use dominant and recessive morphologies at the whole and county levels were estimated by incorporating land use and socio-economic datasets. On this basis, their trade-offs and synergies were qualified through Pearson correlation analysis. The main conclusions are presented as follows:

(1) Bare areas were always the largest land surface cover in the NSTM, and the proportion showed a downward trend over time. The proportion of impervious surfaces gradually and consistently increased from 0.33% in 1990 to 0.77% in 2020. Landscape metrics showed land use structure became more dispersed and fragmented in the past three decades.
(2) More than 20% of the total area in the NSTM experienced land use change from 1990 to 2020. Typically, impervious surfaces were primarily transformed from cropland, bare areas, and grassland, but they were hardly transferred into other land use categories. Bare areas and grassland experienced the large net losses, swap changes, and total changes, while the change rates of impervious surfaces were highest.
(3) Among three land use dominant morphology indices, PD and LSI increased in fluctuation. LPI decreased mainly because vast bare areas transformed into other land use categories. As for land use recessive morphology, LUE, LUI, and ANSP displayed an increasing trend during the past three decades, and this upward trend gradually increased in strength over time.
(4) The strongest trade-off occurred between LSI and LUI, while the synergy between LPI and LUI was strongest. There are significant disparities in terms of spatiotemporal patterns of trade-off and synergetic relationships. The correlation coefficients in different study periods were much smaller than their whole estimations, and the relationships in the eastern NSTM were basically identical with the whole region.

Data availability statement

The original contributions presented in this study are included in the article/supplementary material, further inquiries can be directed to the corresponding author.

Author contributions

HM: conceptualization, methodology, software, validation, formal analysis, investigation, resources, data curation, writing—original draft, review and editing, visualization, and funding acquisition.

Funding

This work was supported by the Third Xinjiang Scientific Expedition Program under Grant 2021xjkk0905.

Acknowledgments

The author grateful to the editor and reviewers for their valuable comments and suggestions.

Conflict of interest

The author declares that the research was conducted in the absence of any commercial or financial relationships that could be construed as a potential conflict of interest.

Publisher's note

All claims expressed in this article are solely those of the authors and do not necessarily represent those of their affiliated organizations, or those of the publisher, the editors and the reviewers. Any product that may be evaluated in this article, or claim that may be made by its manufacturer, is not guaranteed or endorsed by the publisher.

References

An, M., Xie, P., He, W., Wang, B., Huang, J., and Khanal, R. (2022). Spatiotemporal change of ecologic environment quality and human interaction factors in three gorges ecologic economic corridor, based on RSEI. *Ecol. Indic.* 141:109090. doi: 10.1016/j.ecolind.2022.109090

Bai, Y., Li, S., Liu, M., and Guo, Q. (2022). Assessment of vegetation change on the Mongolian Plateau over three decades using different remote sensing products. *J. Environ. Manag.* 317:115509. doi: 10.1016/j.jenvman.2022.115509

Bradford, J. B., and D'Amato, A. W. (2012). Recognizing trade-offs in multi-objective land management. *Front. Ecol. Environ.* 10, 210–216. doi: 10.1890/110031

Buckley Biggs, N. (2022). Drivers and constraints of land use transitions on Western grasslands: insights from a California mountain ranching community. *Landsc. Ecol.* 37, 1185–1205. doi: 10.1007/s10980-021-01385-6

Bukovsky, M. S., Gao, J., Mearns, L. O., and O'Neill, B. C. (2021). SSP-Based Land-Use Change Scenarios: A Critical Uncertainty in Future Regional Climate Change Projections. *Earth Fut.* 9:82. doi: 10.1029/2020EF001782

Cai, E., Liu, Y., Li, J., and Chen, W. (2020). Spatiotemporal Characteristics of Urban–Rural Construction Land Transition and Rural–Urban Migrants in Rapid-Urbanization Areas of Central China. *J. Urban Plann. Dev.* 146:05019023. doi: 10.1061/(ASCE)UP.1943-5444.0000551

Chen, A., Yang, X., Guo, J., Zhang, M., Xing, X., Yang, D., et al. (2022). Dynamic of land use, landscape, and their impact on ecological quality in the northern sand-prevention belt of China. *J. Environ. Manage.* 317:115351. doi: 10.1016/j.jenvman.2022.115351

Clark, M. A., Domingo, N. G. G., Colgan, K., Thakrar, S. K., Tilman, D., Lynch, J., et al. (2020). Global food system emissions could preclude achieving the 1.5° and 2°C climate change targets. *Science* 370, 705–708. doi: 10.1126/science.aba7357

Coomes, O. T., Barham, B. L., MacDonald, G. K., Ramankutty, N., and Chavas, J.-P. (2019). Leveraging total factor productivity growth for sustainable and resilient farming. *Nat. Sustain.* 2, 22–28. doi: 10.1038/s41893-018-0200-3

Cord, A. F., Bartkowski, B., Beckmann, M., Dittrich, A., Hermans-Neumann, K., Kaim, A., et al. (2017). Towards systematic analyses of ecosystem service trade-offs and synergies: Main concepts, methods and the road ahead. *Ecosyst. Serv.* 28, 264–272. doi: 10.1016/j.ecoser.2017.07.012

DeFries, R., Ahuja, R., Friedman, J., Gordon, D. R., Hamburg, S. P., Kerr, S., et al. (2022). Land management can contribute to net zero. *Science* 376, 1163–1165. doi: 10.1126/science.abo0613

Duan, H., Xie, Y., Du, T., and Wang, X. (2021). Random and systematic change analysis in land use change at the category level—A case study on Mu Us area of China. *Sci. Total Environ.* 777:145920. doi: 10.1016/j.scitotenv.2021.145920

Fan, Y., Gan, L., Hong, C., Jessup, L. H., Jin, X., Pijanowski, B. C., et al. (2021). Spatial identification and determinants of trade-offs among multiple land use functions in Jiangsu Province, China. *Sci. Tot. Environ.* 772:145022. doi: 10.1016/j.scitotenv.2021.145022

Foong, A., Pradhan, P., Frör, O., and Kropp, J. P. (2022). Adjusting agricultural emissions for trade matters for climate change mitigation. *Nat. Commun.* 13:3024. doi: 10.1038/s41467-022-30607-x

Fu, F., Deng, S., Wu, D., Liu, W., and Bai, Z. (2022). Research on the spatiotemporal evolution of land use landscape pattern in a county area based on CA-Markov model. *Sustainab. Cities Soc.* 80:103760. doi: 10.1016/j.scs.2022.103760

Fujimori, S., Wu, W., Doelman, J., Frank, S., Hristov, J., Kyle, P., et al. (2022). Land-based climate change mitigation measures can affect agricultural markets and food security. *Nat. Food.* 3, 110–121. doi: 10.1038/s43016-022-00464-4

Geng, W., Li, Y., Zhang, P., Yang, D., Jing, W., and Rong, T. (2022). Analyzing spatio-temporal changes and trade-offs/synergies among ecosystem services in the Yellow River Basin China. *Ecol. Indic.* 138:108825. doi: 10.1016/j.ecolind.2022.108825

Grainger, A. (1995). National Land Use Morphology: Patterns and Possibilities. *Geogr.* 80, 235–245. doi: 10.2307/40572668

Guo, S., and Shen, G. Q. (2015). Multiregional Input–Output Model for China's Farm Land and Water Use. *Environ. Sci. Technol.* 49, 403–414. doi: 10.1021/es503637f

Hamilton, M., Salerno, J., and Fischer, A. P. (2019). Cognition of complexity and trade-offs in a wildfire-prone social-ecological system. *Environ. Res. Lett.* 14:125017. doi: 10.1088/1748-9326/ab59c1

He, F., Yang, J., Zhang, Y., Sun, D., Wang, L., Xiao, X., et al. (2022). Offshore Island Connection Line: A new perspective of coastal urban development boundary simulation and multi-scenario prediction. *GISci. Remote Sens.* 59, 801–821. doi: 10.1080/15481603.2022.2071056

Hong, C., Burney, J. A., Pongratz, J., Nabel, J. E. M. S., Mueller, N. D., Jackson, R. B., et al. (2021). Global and regional drivers of land-use emissions in 1961–2017. *Nature* 589, 554–561. doi: 10.1038/s41586-020-03138-y

Howe, C., Suich, H., Vira, B., and Mace, G. M. (2014). Creating win-wins from trade-offs? Ecosystem services for human well-being: A meta-analysis of ecosystem service trade-offs and synergies in the real world. *Glob. Environ. Change* 28, 263–275. doi: 10.1016/j.gloenvcha.2014.07.005

Howison, R. A., Piersma, T., Kentie, R., Hooijmeijer, J. C. E. W., and Olff, H. (2018). Quantifying landscape-level land-use intensity patterns through radar-based remote sensing. *J. Appl. Ecol.* 55, 1276–1287. doi: 10.1111/1365-2664.13077

Huang, M., Wang, Z., Pan, X., Gong, B., Tu, M., and Liu, Z. (2022). Delimiting China's Urban Growth Boundaries Under Localized Shared Socioeconomic Pathways and Various Urban Expansion Modes. *Earth Fut.* 10:e2021EF002572. doi: 10.1029/2021EF002572

Jiang, H., Sun, Z., Guo, H., Weng, Q., Du, W., Xing, Q., et al. (2021). An assessment of urbanization sustainability in China between 1990 and 2015 using land use efficiency indicators. *NPJ Urban Sustain* 1:34. doi: 10.1038/s42949-021-00032-y

Kubacka, M., Żywica, P., Vila Subirós, J., Bródka, S., and Macias, A. (2022). How do the surrounding areas of national parks work in the context of landscape fragmentation? A case study of 159 protected areas selected in 11 EU countries. *Land Use Policy* 113:105910. doi: 10.1016/j.landusepol.2021.105910

Lausch, A., Blaschke, T., Haase, D., Herzog, F., Syrbe, R.-U., Tischendorf, L., et al. (2015). Understanding and quantifying landscape structure – A review on relevant process characteristics, data models and landscape metrics. *Ecol. Model.* 295, 31–41. doi: 10.1016/j.ecolmodel.2014.08.018

Li, G., Fang, C., Li, Y., Wang, Z., Sun, S., He, S., et al. (2022). Global impacts of future urban expansion on terrestrial vertebrate diversity. *Nat. Commun.* 13:1628. doi: 10.1038/s41467-022-29324-2

Li, H., Peng, J., Liu, Y., and Hu, Y. (2017). Urbanization impact on landscape patterns in Beijing City, China: A spatial heterogeneity perspective. *Ecol. Indic.* 82, 50–60. doi: 10.1016/j.ecolind.2017.06.032

Liu, M., Ma, H., and Bai, Y. (2021). Understanding the Drivers of Land Surface Temperature Based on Multisource Data: A Spatial Econometric Perspective. *IEEE J. Sel. Top. Appl. Earth Observ. Remote Sens.* 14, 12263–12272. doi: 10.1109/JSTARS.2021.3129842

Long, H., and Li, T. (2012). The coupling characteristics and mechanism of farmland and rural housing land transition in China. *J. Geogr. Sci.* 22, 548–562. doi: 10.1007/s11442-012-0946-x

Long, H., Liu, Y., Hou, X., Li, T., and Li, Y. (2014). Effects of land use transitions due to rapid urbanization on ecosystem services: Implications for urban planning in the new developing area of China. *Habitat Int.* 44, 536–544. doi: 10.1016/j.habitatint.2014.10.011

Long, H., Zhang, Y., Ma, L., and Tu, S. (2021). Land Use Transitions: Progress. *Challeng. Prospects. Land* 10:903. doi: 10.3390/land10090903

Ma, L., Bo, J., Li, X., Fang, F., and Cheng, W. (2019). Identifying key landscape pattern indices influencing the ecological security of inland river basin: The middle and lower reaches of Shule River Basin as an example. *Sci. Total Environ.* 674, 424–438. doi: 10.1016/j.scitotenv.2019.04.107

Meng, J., Cheng, H., Li, F., Han, Z., Wei, C., Wu, Y., et al. (2022). Spatial-temporal trade-offs of land multi-functionality and function zoning at finer township scale in the middle reaches of the Heihe River. *Land Use Policy* 115:106019. doi: 10.1016/j.landusepol.2022.106019

Meyfroidt, P., de Bremond, A., Ryan, C. M., Archer, E., Aspinall, R., Chhabra, A., et al. (2022). Ten facts about land systems for sustainability. *Proc. Natl. Acad. Sci. U.S.A.* 119:e2109217118. doi: 10.1073/pnas.2109217118

Müller, S., Gossner, M. M., Penone, C., Jung, K., Renner, S. C., Farina, A., et al. (2022). Land-use intensity and landscape structure drive the acoustic composition of grasslands. *Agricult. Ecosyst. Environ.* 328:107845. doi: 10.1016/j.agee.2021.107845

Ouedraogo, I., Barron, J., Tumbo, S. D., and Kahimba, F. C. (2016). Land Cover Transition in Northern Tanzania. *Land Degrad. Develop.* 27, 682–692. doi: 10.1002/ldr.2461

Plunge, S., Gudas, M., and Povilaitis, A. (2022). Effectiveness of best management practices for non-point source agricultural water pollution control with changing climate – Lithuania's case. *Agricult. Water Manag.* 267:107635. doi: 10.1016/j.agwat.2022.107635

Qu, Y., Shu, Y., Zong, H., Si, H., Yang, Z., and Liu, T. (2021). Understanding the Characteristics and Realization Path of Urban Land Use Transition in the Bohai Economic Rim: An Analytical Framework of "Dominant–Recessive" Morphology Coupling. *Land* 10:493. doi: 10.3390/land10050493

Ray, D. K., Sloat, L. L., Garcia, A. S., Davis, K. F., Ali, T., and Xie, W. (2022). Crop harvests for direct food use insufficient to meet the UN's food security goal. *Nat. Food* 3, 367–374. doi: 10.1038/s43016-022-00504-z

Ren, J., Yang, J., Zhang, Y., Xiao, X., Xia, J. C., Li, X., et al. (2022). Exploring thermal comfort of urban buildings based on local climate zones. *J. Clean. Product.* 340:130744. doi: 10.1016/j.jclepro.2022.130744

Schiavina, M., Melchiorri, M., Freire, S., Florio, P., Ehrlich, D., Tommasi, P., et al. (2022). Land use efficiency of functional urban areas: Global pattern and evolution of development trajectories. *Habitat Int.* 123:02543. doi: 10.1016/j.habitatint.2022.102543

Searchinger, T. D., Wirsenius, S., Beringer, T., and Dumas, P. (2018). Assessing the efficiency of changes in land use for mitigating climate change. *Nature* 564, 249–253. doi: 10.1038/s41586-018-0757-z

Sumari, N. S., Cobbinah, P. B., Ujoh, F., and Xu, G. (2020). On the absurdity of rapid urbanization: Spatio-temporal analysis of land-use changes in Morogoro, Tanzania. *Cities* 107:102876. doi: 10.1016/j.cities.2020.102876

Tan, L. M., Arbabi, H., Densley Tingley, D., Brockway, P. E., and Mayfield, M. (2021). Mapping resource effectiveness across urban systems. *NPJ Urban Sustain* 1, 1–14. doi: 10.1038/s42949-020-00009-3

Tan, S., Liu, Q., and Han, S. (2022). Spatial-temporal evolution of coupling relationship between land development intensity and resources environment carrying capacity in China. *J. Environ. Manag.* 301:113778. doi: 10.1016/j.jenvman.2021.113778

van Marle, M. J. E., van Wees, D., Houghton, R. A., Field, R. D., Verbesselt, J., and van der Werf, G. R. (2022). New land-use-change emissions indicate a declining CO2 airborne fraction. *Nature* 603, 450–454. doi: 10.1038/s41586-021-04376-4

Wang, R., Bai, Z., Chang, J., Li, Q., Hristov, A. N., Smith, P., et al. (2022). China's low-emission pathways toward climate-neutral livestock production for animal-derived foods. *Innovation* 3:100220. doi: 10.1016/j.xinn.2022.100220

Wu, J., and Lu, J. (2021). Spatial scale effects of landscape metrics on stream water quality and their seasonal changes. *Water Res.* 191:116811. doi: 10.1016/j.watres.2021.116811

Wu, Y., Xi, X., Tang, X., Luo, D., Gu, B., Lam, S. K., et al. (2018). Policy distortions, farm size, and the overuse of agricultural chemicals in China. *Proc. Natl. Acad. Sci.U.S.A.* 115, 7010–7015. doi: 10.1073/pnas.1806645115

Xu, F., Wang, Z., Chi, G., and Zhang, Z. (2020). The impacts of population and agglomeration development on land use intensity: New evidence behind urbanization in China. *Land Use Policy* 95:104639. doi: 10.1016/j.landusepol.2020.104639

Yang, J., Guo, A., Li, Y., Zhang, Y., and Li, X. (2019). Simulation of landscape spatial layout evolution in rural-urban fringe areas: a case study of Ganjingzi District. *GISci. Remote Sens.* 56, 388–405. doi: 10.1080/15481603.2018.1533680

Yang, J., Yang, R., Chen, M.-H., Su, C.-H., Zhi, Y., and Xi, J. (2021). Effects of rural revitalization on rural tourism. *J. Hospital. Tourism Manag.* 47, 35–45. doi: 10.1016/j.jhtm.2021.02.008

Yin, G., Lin, Z., Jiang, X., Qiu, M., and Sun, J. (2020). How do the industrial land use intensity and dominant industries guide the urban land use? Evidences from 19 industrial land categories in ten cities of China. *Sustainab. Cities Soc.* 53:101978. doi: 10.1016/j.scs.2019.101978

Yu, J., Zhou, K., and Yang, S. (2019). Land use efficiency and influencing factors of urban agglomerations in China. *Land Use Policy* 88:104143. doi: 10.1016/j.landusepol.2019.104143

Zhang, X., Liu, L., Chen, X., Gao, Y., Xie, S., and Mi, J. (2021). GLC_FCS30: global land-cover product with fine classification system at 30 m using time-series Landsat imagery. *Earth Syst. Sci. Data* 13, 2753–2776. doi: 10.5194/essd-13-2753-2021

Zhang, Y., Long, H., Li, Y., Tu, S., and Jiang, T. (2021). Non-point source pollution in response to rural transformation development: A comprehensive analysis of China's traditional farming area. *J. Rural Stud.* 83, 165–176. doi: 10.1016/j.jrurstud.2020.10.010

Zhou, Q., Zhang, Y., Tao, J., Ye, L., Wang, H., Shan, K., et al. (2022). Water depth and land-use intensity indirectly determine phytoplankton functional diversity and further regulate resource use efficiency at a multi-lake scale. *Sci. Total Environ.* 834:155303. doi: 10.1016/j.scitotenv.2022.155303

Zhu, C., Dong, B., Li, S., Lin, Y., Shahtahmassebi, A., You, S., et al. (2021). Identifying the trade-offs and synergies among land use functions and their influencing factors from a geospatial perspective: A case study in Hangzhou, China. *J. Clean. Product.* 314:128026. doi: 10.1016/j.jclepro.2021.128026

Zuo, L., Zhang, Z., Carlson, K. M., MacDonald, G. K., Brauman, K. A., Liu, Y., et al. (2018). Progress towards sustainable intensification in China challenged by land-use change. *Nat. Sustain* 1, 304–313. doi: 10.1038/s41893-018-0076-2